

GMD 2022 Feb 08 15:14:53

Figure 1: (Left) Larger-scale bird's eyes perspective of 250 MHz GPR, 50 MHz GPR, static & polarimetric (SPM) and continuous ApRES (cApRES) locations at Ekström Ice Shelf, East Antarctica. (Right) Close-up of the survey grid close to the grounding-zone.

## 1 Summary of ReMeltRadar 2021/22

### RD

ReMeltRadar's scientific focus (1) to understand & quantify processes that govern ocean-induced melting at the base of ice shelves, and (2) to provide observational constraints on the spatial variability of ice rheology impacting ice-shelf buttressing strength. The area of interest is the Ekström Ice Shelf, East Antarctica, using the Neuyamer III station as a logistical hub for field surveys on the ice shelf and in the grounding zone. The first field season took place from November 2021 to January 2022. This report details the data collected and will serve as a baseline for envisaged repeat measurements in 2022/23.

Name	Project	Deployment	Responsibility
Inka Koch (UT)	ReMeltRadar	27.12.21-13.12.22	PulseEkko GPR
Jonathan Hawkins (UCL)	ReMeltRadar	27.12.21-13.12.22	HF ApRES
Reinhard Drews (UT)	ReMeltRadar	27.12.21-13.12.22	Science Coordination
Reza Ershadi (UT)	ReMeltRadar	05.11.21-13.12.22	Rover, SPM
Olaf Eisen (AWI)	ReMeltRadar	05.11.21-13.12.22	Traverse Leader

Table 1: Team composition of ReMeltRadar with members of University of Tübingen (UT), University College London (UCL), and Alfred Wegener Institute (AWI).

## 1.1 Team composition and chronology of data collection

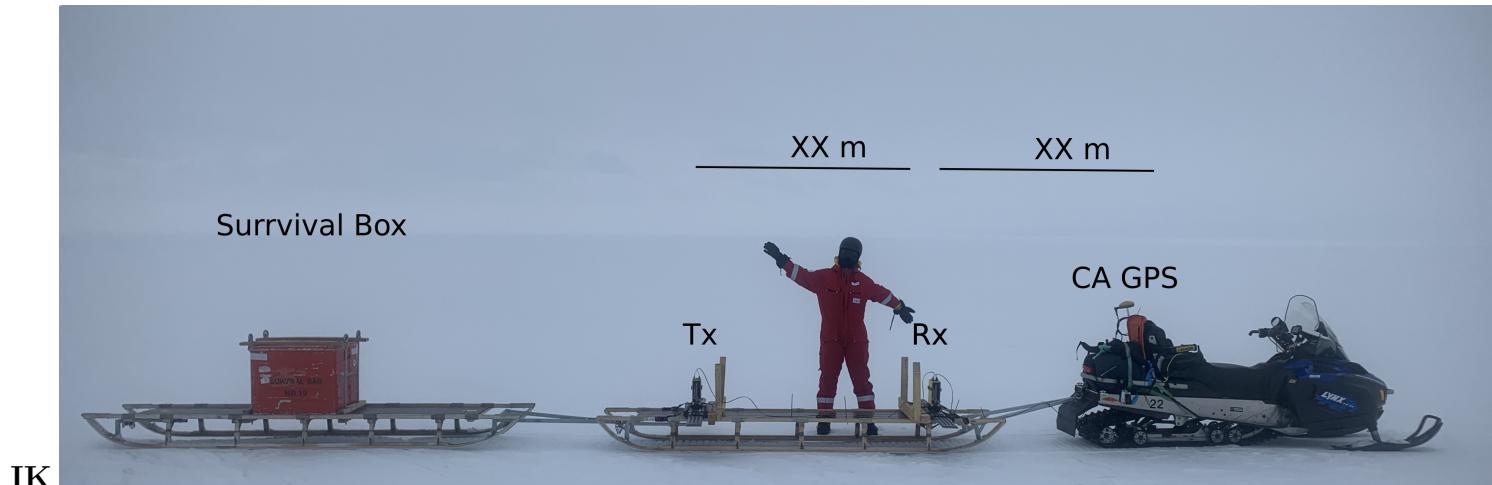
Date	Frequency	Profile	File-ID
28.12.21	50, 100 MHz	Test profiles near NM	<i>PE files</i>
29.12.21	100 MHz	MPA01-MPA03, SPX4-SPX2 near NM	<i>PE files</i>
01.01.22	250 MHz	NM-SPMA25 during traverse	<i>PE files</i>
02.01.22	50 MHz	GZ profiling along flow (SPMA25-SPMA21-GLPE3n-GLPE4s)	<i>PE files</i>
03.01.22	50 MHz	GZ profiling along flow (GLPE4s-GLPE1s-GLPE2n transfer to SPMA25)	<i>PE files</i>
04.01.22	50 MHz	GZ profiling along flow (GLPE7n-GLPE8s-GLPE5s)	<i>PE files</i>
05.01.22	50 MHz	GZ profiling across flow (XX points XX)	<i>PE files</i>
06.01.22	50 MHz	Finegrid along flow (XX points XX)	<i>PE files</i>
09.01.22	50 MHz	Finegrid across flow (XX points XX)	<i>PE files</i>
10.01.22	50 MHz	Along-flow Camp-NM (SPMA21-SPMA10)	<i>PE files</i>
12.01.22	50 MHz	Camp-NM continuation (SPMA10 - XX)	<i>PE files</i>

Table 2: Overview of GPR measurements taken with the PulseEkko radar from Sensors&Software. Details for the system setup and individual profiles are found in Section 3. Operator: I. Koch.  
Here we need a table such as table for each sensor.

## 2 Data structure and initial source codes

RD, JH

### 3 GPR: Data example, field picture, system setup and profile specifics



## 4 SPM: Data example, field picture, system setup and site specifics

RE

## 5 HF ApRES

### 5.1 System Overview

The HF ApRES is a frequency modulated continuous wave (FMCW) radar operating over a bandwidth of 20 MHz to 40 MHz. It builds upon the existing phase-coherent radar architecture of the ApRES<sup>1</sup> but uses a modified radio front-end to operate at the reduced bandwidth described. In addition to the radar, the HF ApRES makes use of two 'wire-mesh dipole' antennas - one each for the transmitter and receiver, and a 12V 7 A h lead-acid battery for power. Testing was required to validate the performance of both the HF ApRES radar unit and 'wire-mesh dipole' antennas, as they had not been previously deployed on a polar ice shelf and subject only to verification through simulation and laboratory testing.

#### 5.1.1 System Equipment Listing

- 1x HF ApRES (VAB Issue C and RMB2F in Pelicase)
- 2x Wire-Mesh Dipole Antennas
- Clusons 12V 7 A h Lead Acid Battery
- 4x Radiall RG213 5 m 50Ω RF Cables (R284C0351044)
- 2x Gigatronix LBC400 25 m 50Ω RF Cables (APX2KDP6ZAB40L)
- 2x 10 dB RF attenuators
- Various RF connectors
- Trimble R9s Modular GNSS System (receiver and base station with UHF radio link)
- Bamboo and 10mm kernmantle rope for towed configuration.

### 5.2 Testing Summary

Testing was first conducted with the wire-mesh antennas to verify that they met the power transfer characteristics predicted through simulation. Once verified, a setup with the full HF ApRES system was configured and issues were found with strong coupling between the transmit and receive antennas. After further testing, it was found that broadside orientation of the antennas and increased separation reduced the direct coupling between the antennas sufficiently for clean deramped signals to be recorded.

---

<sup>1</sup>P. Brennan, L. Lok, K. Nicholls and H. Corr, "Phase-sensitive FMCW radar system for high-precision Antarctic ice shelf profile monitoring", IET Radar, Sonar & Navigation, vol. 8, no. 7, pp. 776-786, 2014. Available: 10.1049/iet-rsn.2013.0053.

Date	Frequency	Profile	File-ID
27.12.21	30 MHz	Testing of antennas and HF ApRES near Neumayer	<i>Testing.db</i>
28.12.21	30 MHz	(as above)	<i>Testing.db</i>
29.12.21	30 MHz	(as above)	<i>Testing.db</i>
30.12.21	30 MHz	(as above)	<i>Testing.db</i>
02.01.22	30 MHz	Testing of HF ApRES at Camp	<i>Testing.db</i>
03.01.22	30 MHz	(as above)	<i>Testing.db</i>
04.01.22	30 MHz	(as above)	<i>Testing.db</i>
05.01.22	30 MHz	(as above)	<i>Testing.db</i>
06.01.22	30 MHz	Testing of HF ApRES at Camp and relocate to GL	<i>Testing.db</i>
07.01.22	30 MHz	Initial measurements of start-stop survey at GL	<i>Testing.db,</i> <i>StartStop.db</i>
08.01.22	30 MHz	Complete measurement of start-stop survey at GL and attempt kinematic surveys	<i>Testing.db,</i> <i>StartStop.db</i>

Table 3: Overview of measurements taken with HF ApRES System



Figure 2: Deployed HF ApRES radar positioned in centre of transmit (Tx) and receive (Rx) antennas in endfire configuration.

### Wire-Mesh Dipole Antennas

The wire-mesh dipole antennas were each tested with an SDRKits Vector Network Analyzer (VNA) which allows for the measurement of the antenna reflection coefficient ( $\Gamma$ ). The reflection coefficient is calculated from the scattering parameters (s-parameters) measured by the VNA, where  $S_{11}$  refers to the phasor ratio between the scattered and incident voltages from the antenna. The reflection coefficient can therefore be used to infer the ratio of incident power to the antenna which is 'accepted' and sets an upper bound on the radiation efficiency. The radiation efficiency of the antenna is the ratio of incident power to the antenna that is actually radiated rather than scattered back to the radar, or lost through conduction within the antenna structure. Radiation efficiency is difficult to measure in a field environment, hence the reflection coefficient is used to determine an upper bound.

$$|\Gamma|_{\text{dB}} = 20 \log_{10} |S_{11}| \quad (1)$$

The measured reflection coefficient of the wire-mesh dipole antennas from tests on 28.12.21 is shown in Figure 3. Within the field of antenna engineering, a reflection coefficient of less than  $-10 \text{ dB}$  across the desired signal bandwidth, i.e. greater than 90% of power accepted by the antenna, is deemed to be acceptable. It can be seen that during initial tests conducted 500 m south-west of Neumayer Station the antennas have a measured  $|S_{11}|_{\text{dB}}$  of less than  $-10 \text{ dB}$  across the desired signal bandwidth of 20 MHz to 40 MHz. Discussion regarding the antenna orientation can be found in Section ???.

**Note:** After transport of the antennas from Neumayer III to the grounding line camp, it was found that one of the centre-pin conductors on the antenna arms had become loose, likely due to a dry solder joint.

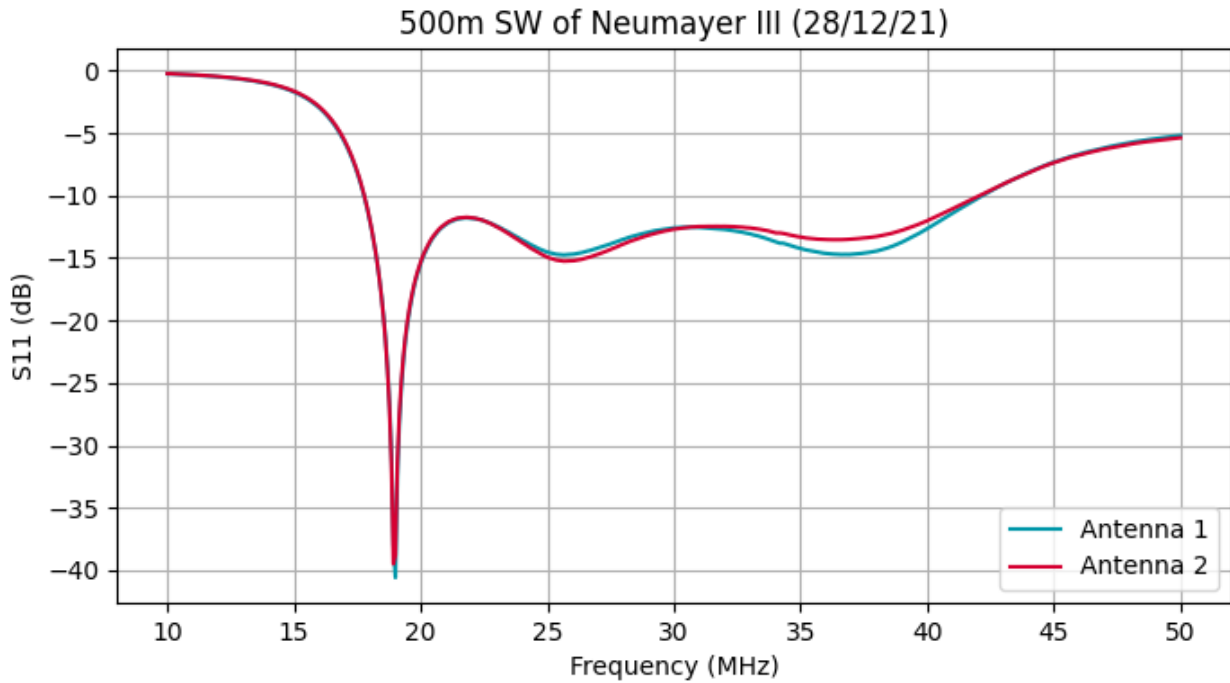


Figure 3: Measured power reflection coefficient for HF wire-mesh dipole antennas, positioned approximately 500 m south-west of Neumayer Station.

## HF ApRES Radar

Figure 4 shows a measured test profile at Neumayer Station where it was discovered that the receiving antenna of the HF ApRES radar was disconnected. A radar echo from is visible at approximately 250 m depth, which corresponds with the expected thickness of the ice shelf in the vicinity of the station. The working explanation for the clear, high signal-to-noise ratio (SNR) echo from the ice-shelf base with no receiving antenna is that the echo is received by the transmitting antenna and coupled to the mixer through the ADP-2-1W power divider to the ADE-1HW mixer, shown in Figure 4.

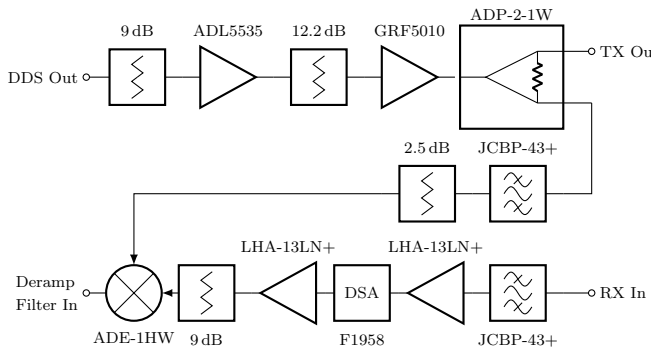


Figure 4: System level diagram of the RMB2F radar, showing the signal path from the direct digital synthetiser (DDS) to the transmit output, receiver input and ouput deramped FMCW signal.

Reconnecting the receiver antenna, as shown in Figure 5 results in significant distortion visible in the time-domain FMCW voltage signal, matched with the reduced SNR seen in the range-power profile. Overall power is increased relative to Figure 4, which gives confidence that the antenna was not connected and has been successfully reconnected in the second dataset. The distortion is characteristic of 'clipping' where the recorded signal exceeds the voltage range of the analogue-to-digital converter and the output is subsequently 'clipped' to be within this range. The evidence of clipping, at low frequencies corresponding to short range echoes suggests that the direct coupling between the antennas is higher than experienced from a previous deployment of the HF ApRES radar on an Alpine glacier.

**Antenna orientation** was shown to be related to the coupling between the transmit and receive antennas and the presence of high-power low frequency signals in the deramped FMCW voltage signal. Broadside refers to the antennas positioned such that their phase centres are in line with the survey direction and their longest axes are orthogonal to the survey direction. Endfire refers to the antennas positioned such that their longest axes are parallel to the survey direction. Experiments repeated at Neumayer Station and the grounding line camp show that these antennas are aligned in a 'broadside' configuration they exhibit reduced near-range coupling compared to antennas separated by the same distance in an 'endfire' configuration. The HF ApRES was then reconfigured to be operated with the SubZero rover in a broadside configuration, with an increased separation between the transmit and receive antennas of 40 m.

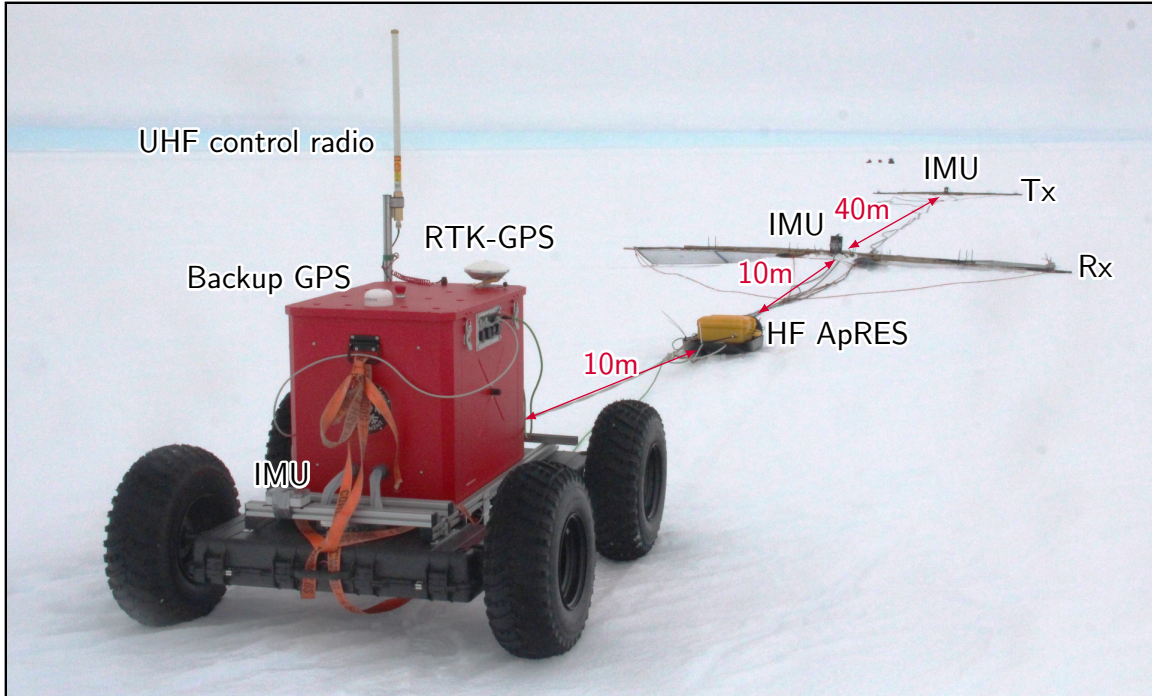
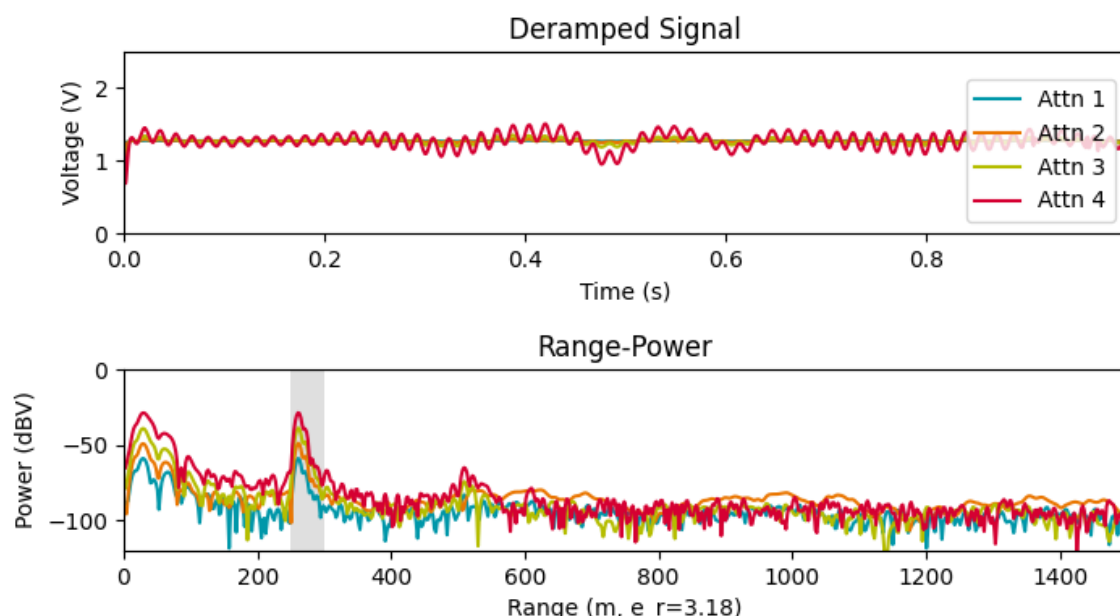


Figure 5: SubZero rover and HF ApRES configuration used for start-stop and kinematic synthetic aperture radar acquisitions at grounding line.

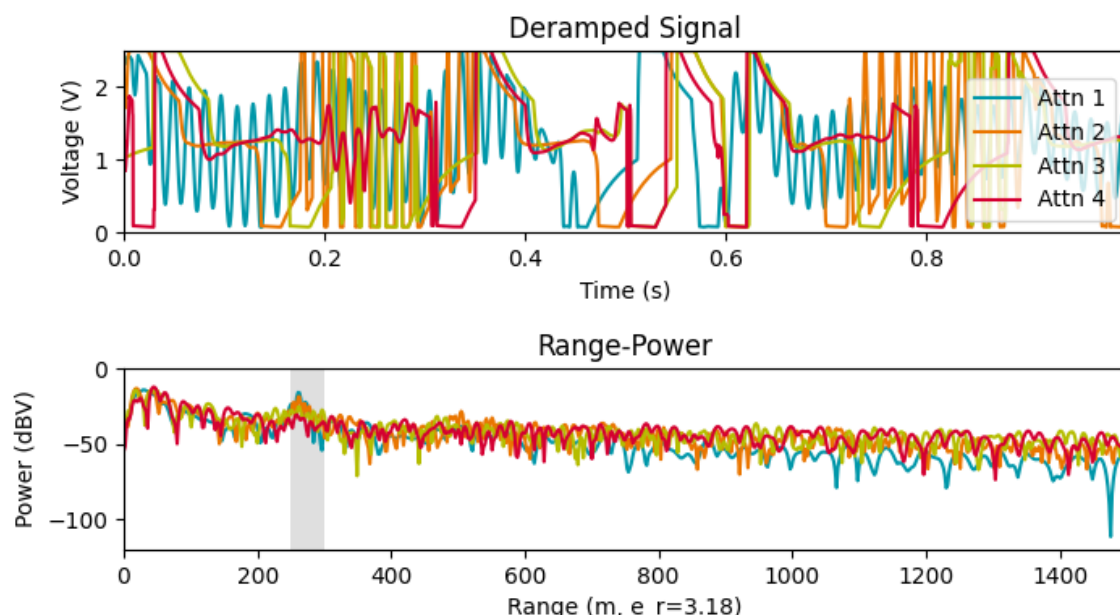
Table 4: Antennas aligned E-W, no receive antenna connected but clear return from ice-shelf base and double bounce.



**Filename** 2021-12-28\_213752.dat

Param.	Value	Param.	Value
<b>AF Gain</b>	6,6,6,6	<b>RF Attn.</b>	30,20,10,0
<b>Subbursts</b>	10	<b>Period (<math>T</math>)</b>	1.000 s
<b>Bandwidth</b>	20 - 40 MHz	<b>Power Code</b>	127
<b>Batt. Volt.</b>	12.129 V	-	-

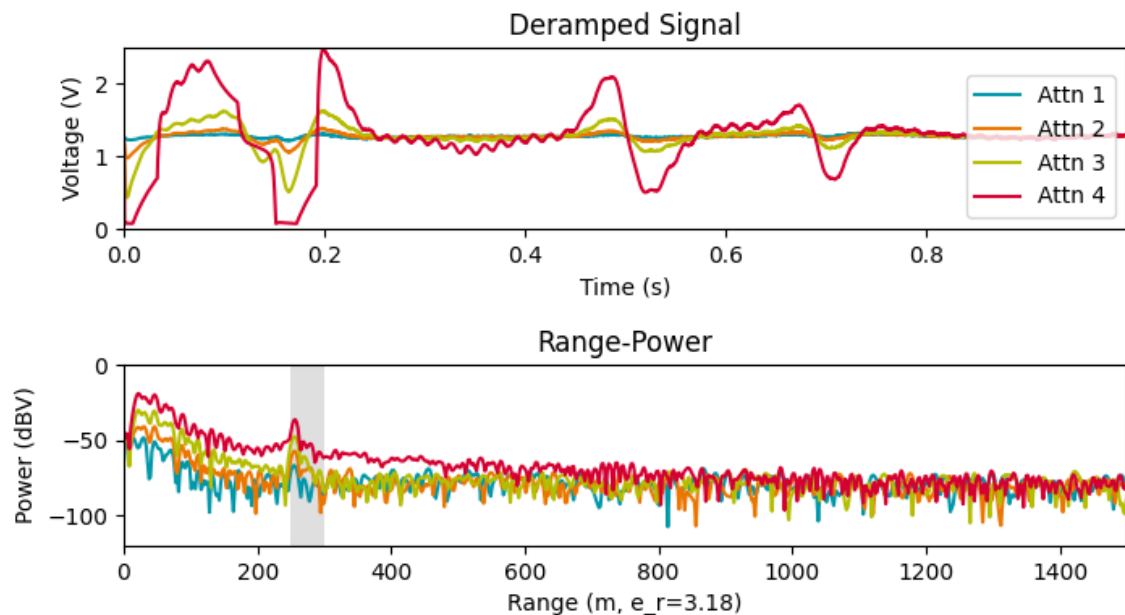
Table 5: Antennas aligned E-W, receive antenna reconnected and low-frequency (i.e. near range) distortion present in signal resulting in reduced signal-to-noise ratio.



**Filename** 2021-12-28\_214326.dat

Param.	Value	Param.	Value
<b>AF Gain</b>	6,6,6,6	<b>RF Attn.</b>	30,20,10,0
<b>Subbursts</b>	10	<b>Period (<math>T</math>)</b>	1.000 s
<b>Bandwidth</b>	20 - 40 MHz	<b>Power Code</b>	127
<b>Batt. Volt.</b>	12.158 V	-	-

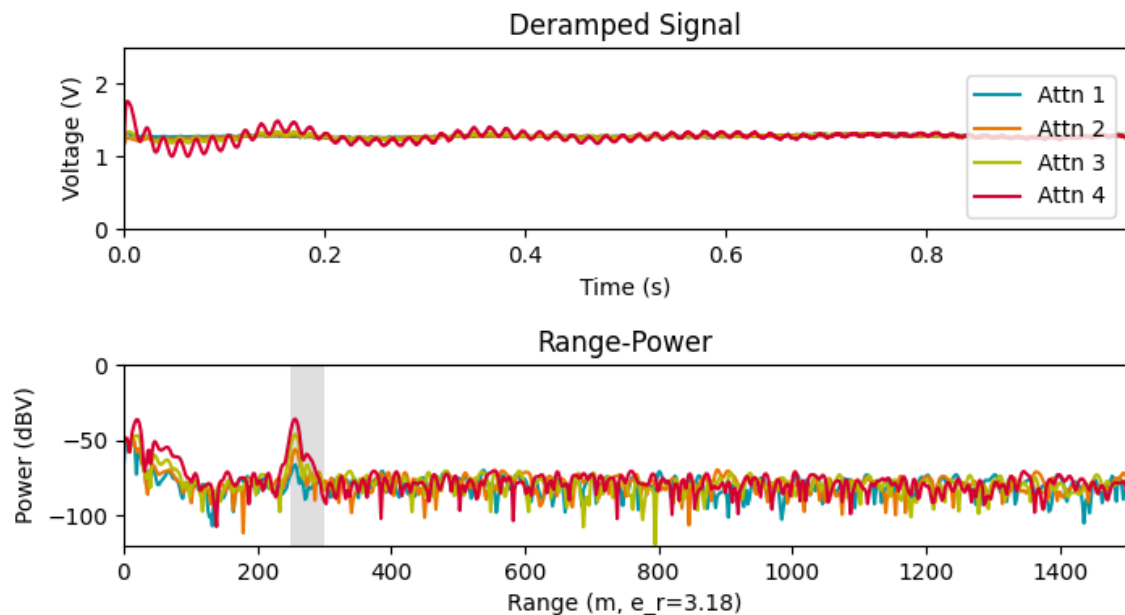
Table 6: **Antenna Orientation: Endfire, Neumayer.** No additional attenuations. Antennas rotated so they are aligned N-S and cables N-S. Similar to above but with noise in upper layers. 14m separation. Cables 'smooth' in line with antennas. Reduced power code to 0.



**Filename** 2021-12-29\_215659.dat

Param.	Value	Param.	Value
AF Gain	6,6,6,6	RF Attn.	30,20,10,0
Subbursts	1	Period ( $T$ )	1.000 s
Bandwidth	20 - 40 MHz	Power Code	0
Batt. Volt.	12.266 V	-	-

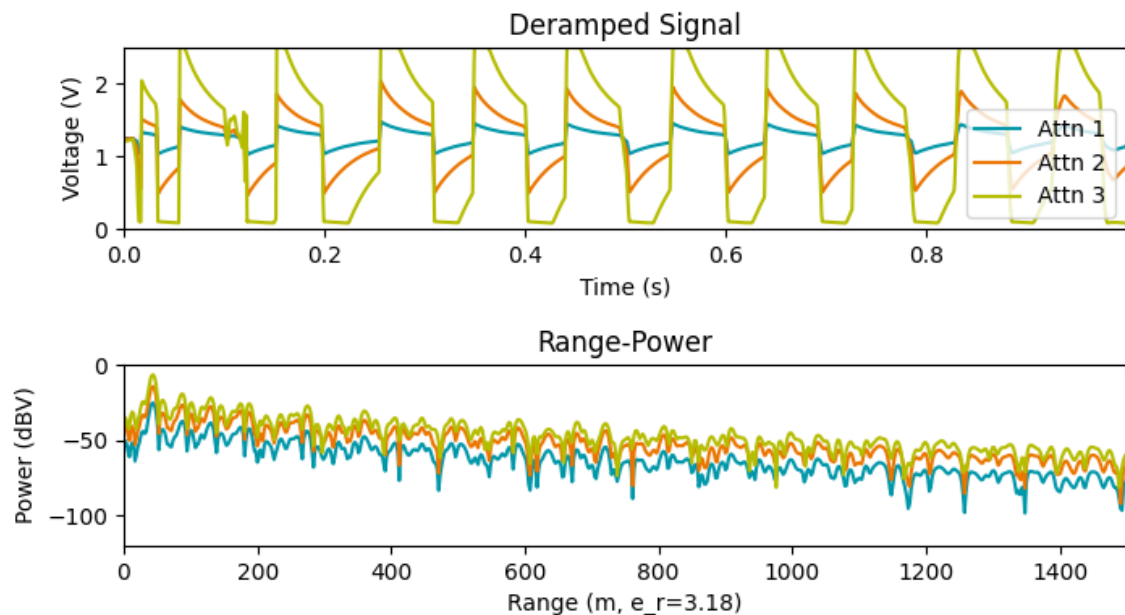
Table 7: **Antenna Orientation: Broadside, Neumayer.** No additional attenuations. Antennas rotated so they are aligned E-W but Tx at N and Rx at S. Similar to above but with noise in upper layers. 14m separation. Cables 'smooth' in line with antennas. Reduced power code to 0.



**Filename** 2021-12-29\_220442.dat

Param.	Value	Param.	Value
<b>AF Gain</b>	6,6,6,6	<b>RF Attn.</b>	30,20,10,0
<b>Subbursts</b>	1	<b>Period (<math>T</math>)</b>	1.000 s
<b>Bandwidth</b>	20 - 40 MHz	<b>Power Code</b>	0
<b>Batt. Volt.</b>	12.258 V	-	-

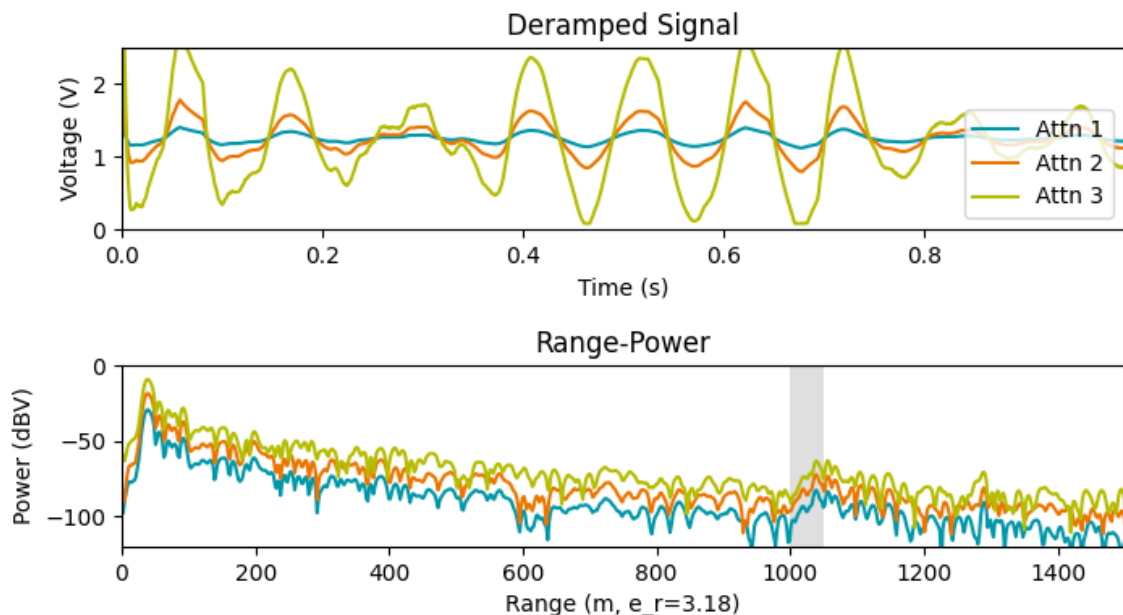
Table 8: **Antenna Orientation: Endfire, Grounding Line.** Additional attenuator 10dB Rx, 0dB Tx. Cable length Tx 25m, Rx 25m and separate antennas to maximum length (30m). Antennas return to endfire. Clipping across all AF settings. No clear basal return.



**Filename** 2022-01-05\_174254.dat

Param.	Value	Param.	Value
<b>AF Gain</b>	-14,-4,6	<b>RF Attn.</b>	0,0,0
<b>Subbursts</b>	40	<b>Period (T)</b>	1.000 s
<b>Bandwidth</b>	20 - 40 MHz	<b>Power Code</b>	127
<b>Batt. Volt.</b>	12.238 V	-	-

Table 9: **Antenna Orientation: Broadside, Grounding Line.** Additional attenuator 10dB Rx, 0dB Tx. Increase Tx cable to 25m (Rx 5m) and separate antennas to maximum length (30m). Antennas rotated broadside. Bed clearer (higher SNR)? Some clipping in signal. Repeated as before - ringing reduced?



**Filename** 2022-01-05\_171029.dat

Param.	Value	Param.	Value
<b>AF Gain</b>	-14,-4,6	<b>RF Attn.</b>	0,0,0
<b>Subbursts</b>	40	<b>Period (<math>T</math>)</b>	1.000 s
<b>Bandwidth</b>	20 - 40 MHz	<b>Power Code</b>	127
<b>Batt. Volt.</b>	12.238 V	-	-

### 5.3 Synthetic Aperture Radar Measurements

The test site chosen for the HF ApRES SAR measurements was selected to coincide with the series of basal terraces observed in the PulseEKKO data located in the finely gridded region of Figure 1. The HF ApRES system was towed into position on 7<sup>th</sup> January, configured according to 5 and initial testing was conducted, including the resolution of a software navigation issue with the rover. Two modes of measurement were conducted with the HF ApRES: a start-stop profile where the instrument was repositioned in steps of 1 m increments along the desired profile direct, and kinematic profiles where the radar was set to continuously measure while towed along the profile by the SubZero rover at speeds of approximately  $0.7 \text{ m s}^{-1}$  to  $1 \text{ m s}^{-1}$ . For all measurement modes, the radar was configured with the parameters listed in Table 10. The VV notation for the polarisation is consistent with that of the rover-towed VHF system, however the precise polarisation response of the wire-mesh dipole antennas has not been measured.

Parameter	Symbol	Value	
Centre Frequency	$f_c$	30	MHz
Bandwidth	$B$	20	MHz
Pulse Duration	$T$	1	s
Transmit Power	$P_T$	0.1	W
AF Gain	$G_{AF}$	6	dB
RF Attenuation	$A_{RF}$	10	dB
RF Atten. (External)	$A_{RFExt}$	10	dB
Antenna Separation	$S_{Ant}$	40	m
Rover Separation	$S_{Rov}$	10	m
Polarisation	-	VV	-

Table 10: Radar configuration parameters common to both the start-stop and kinematic the HF ApRES SAR measurements

#### 5.3.1 Start-Stop Measurement

On the 7<sup>th</sup> January, 192 m of the intended profile was covered . The rover was left in position overnight and the profile was resumed to cover the remaining 710 m over approximately 5 hours, including approximately

one hour of cumulative downtime. The Trimble R9s base station was set up approximately 40 m away from the profile at its centre. The RINEX files generated by the GNSS receivers at the base station and on the rover were processed using the Canadian Spatial Reference System Precise Point Positioning service<sup>2</sup> and are shown in Figure 8. There are tidal and ice flow components present in the raw position data. The ice velocity ( $v$ ) is assumed constant along the length of the profile from analysis of the 120 m composite ITS\_LIVE data for 2020. The tidal components of the measured elevation were analysed using the Tidal Fitting Toolbox <sup>3</sup> but have not yet been validated with external data. It is assumed that the tidal components are also locally invariant and therefore the relative position of the rover to the base is initially found through subtraction of the base station coordinates from the rover coordinates. Phase and power of raw data is shown in Figure 6.

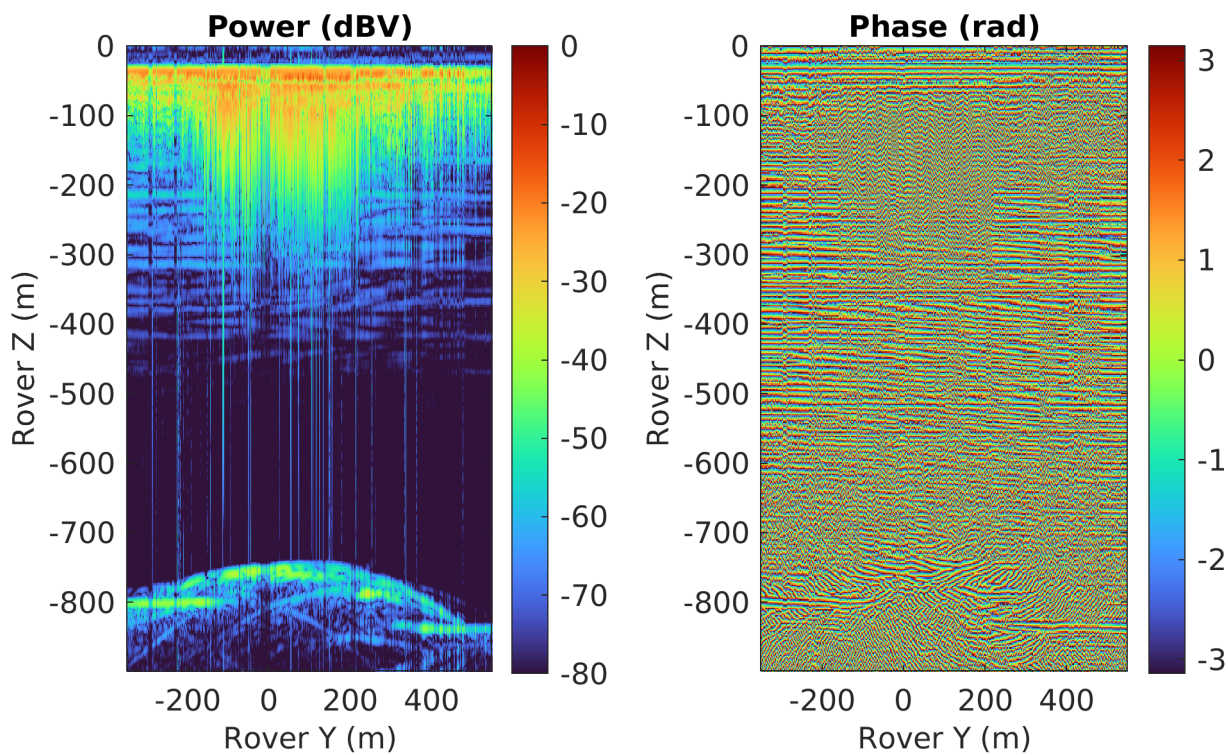


Figure 6: Phase and power of raw, unprocessed ApRES data collected along the profile.

Initial SAR processing of the dataset was performed using an interpolated sinc routine using the MATLAB<sup>®</sup> ApRESProcessor library<sup>4</sup> with a constant velocity travel-time model using a dielectric permittivity for ice of 3.15. Antenna positions were modelled to be 50 m and 10 m behind the rover, in the direction of the image plane, as per the system setup indicated in Figure 5. For the intial pass, bursts with low signal to noise ratios compared to the mean of the dataset were excluded however further passes will select

<sup>2</sup>Full details can be found in `Raw/RTKGPS/ApRES/Rover/HF/processing_notes.md`

<sup>3</sup><https://uk.mathworks.com/matlabcentral/fileexchange/19099-tidal-fitting-toolbox>

<sup>4</sup><https://github.com/jonodhawkins/apresprocessor>

individual chirps from these bursts to maximise the number of radar locations at which the backprojection is performed. Results of the backprojection in power and phase are shown in Figure 7.

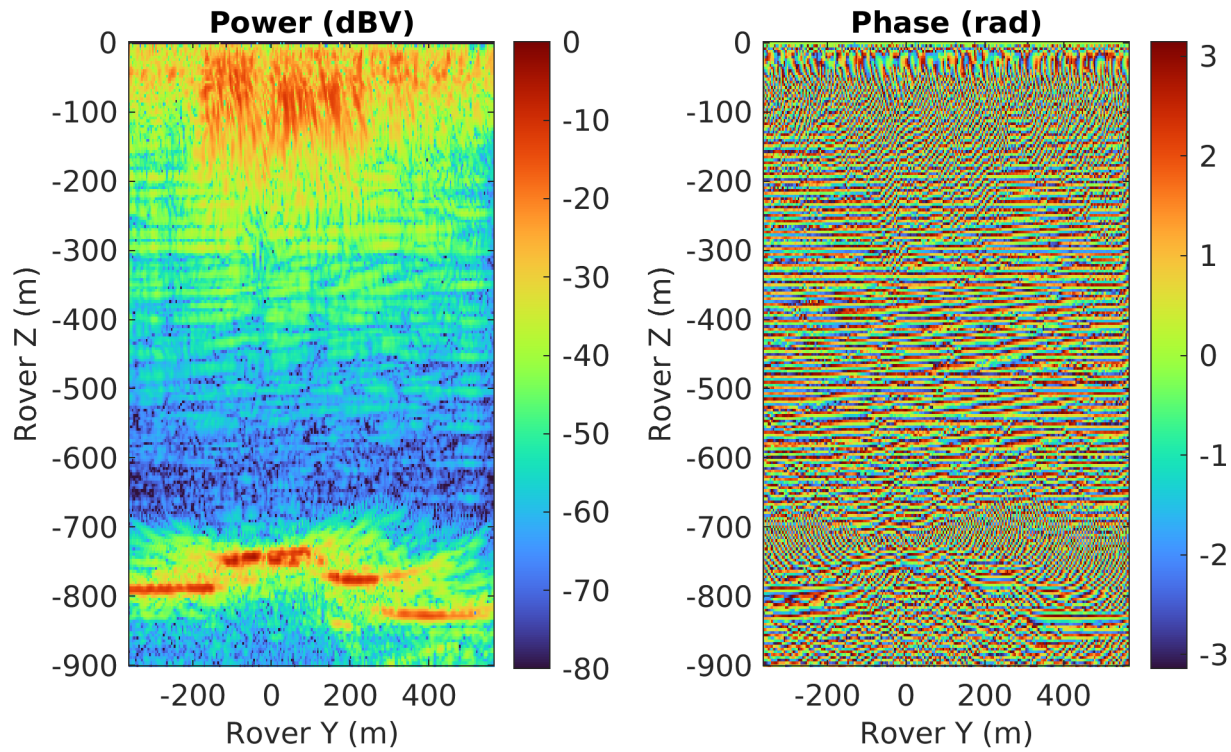


Figure 7: Phase and power of initial backprojected (SAR processed) image from the HF ApRES towed by the SubZero rover. The coordinate system for the image is relative polar stereographic to the Trimble GPS base station. Pixel resolution is 4 m.

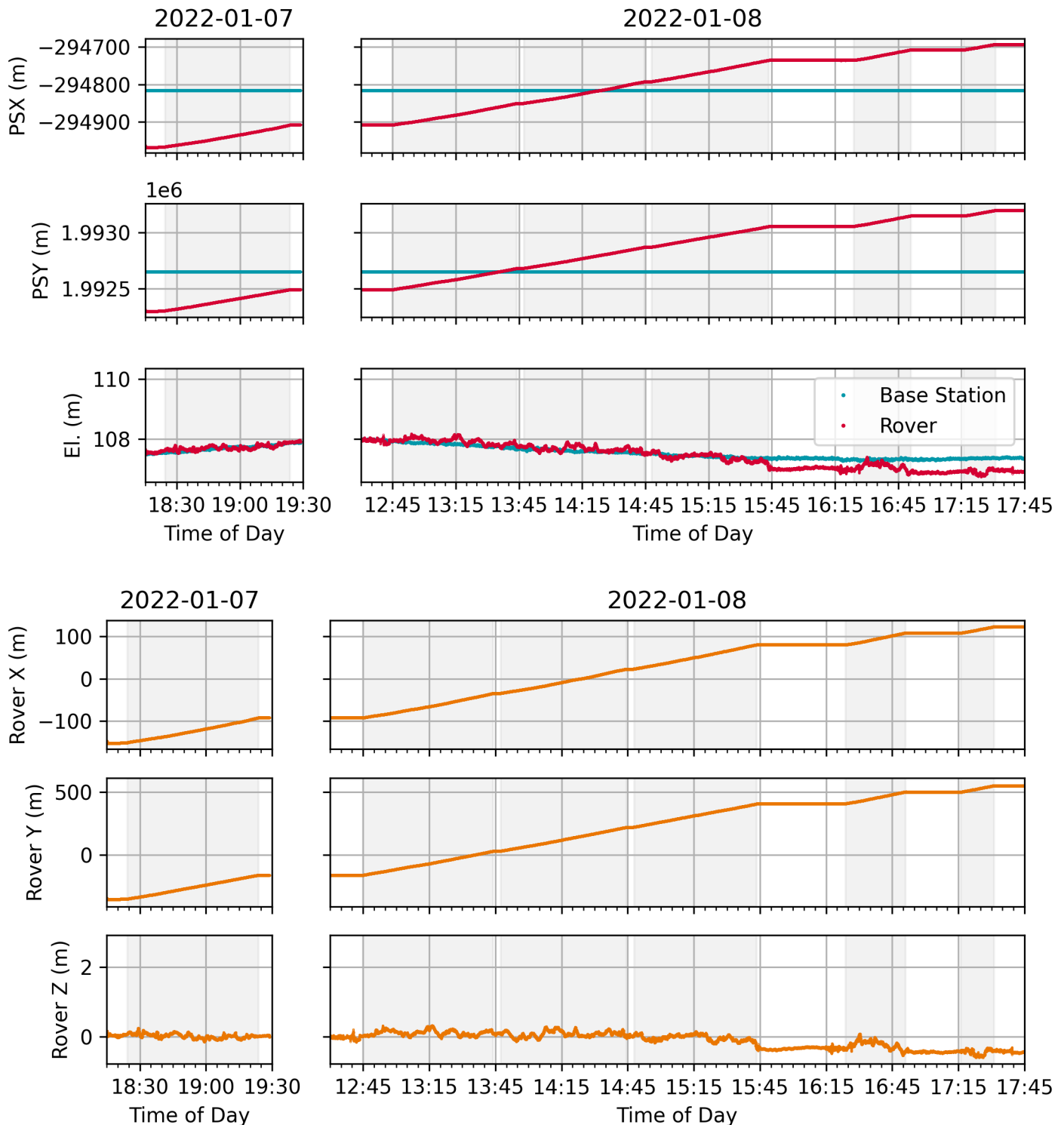


Figure 8: Precise point positioned GPS outputs from Canadian Spatial Reference System for rover and base station. Gray highlighted areas show periods of rover operation. Second plot shows derived relative position of rover to base station, mitigating tidal flexure of ice shelf and positional drift from ice flow.

## 6 cApRES: Data example, field picture, system setup and site specifics

RE,JH

## 7 Rover-ApRES: Data example, field picture, system setup and site specifics

RE